

Research Article

Mild Steel Corrosion Inhibition Capacity of Schiff Base Derived from Thiophene-2-Carbaldehyde: Gravimetric and Electrochemical Investigation

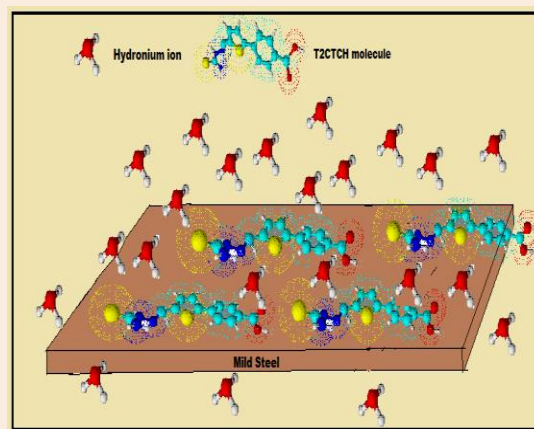
Nimmy Kuriakose, Joby Thomas K*, Vinod P Raphael, Shaju K S

St.Thomas' College (University of Calicut) Thrissur, Kerala, India

Abstract

The corrosion inhibition efficiency of thiophene-2-carbaldehydethiocarbamoyl hydrazide (T2CTCH) on mild steel (MS) in 1M HCl solution has been investigated and compared using weight loss measurements, electrochemical impedance spectroscopy and potentiodynamic polarization analysis. The inhibitor exhibited marked corrosion inhibition on mild steel in HCl medium and the inhibition efficiency increased with the increase in concentration. The adsorption of the inhibitor on the surface of the corroding metal obeys Langmuir isotherm. Thermodynamic parameters (K_{ads} , ΔG_{ads}) were calculated using adsorption isotherm. A maximum of 94.69% inhibition efficiency was achieved by EIS studies at a concentration of 1mM. Polarization studies revealed that T2CTCH acts as a mixed type inhibitor.

Keywords: Thiophene-2-carbaldehyde, Corrosion inhibitor, Schiff base, EIS, Polarization inhibitor

***Correspondence**

Joby Thomas,
Email: drjobythomask@gmail.com

Introduction

Nitrogen containing organic compounds are well known as efficient corrosion inhibitors in acid solutions [1-5]. The compounds rich in hetero atoms are considered as environmental friendly inhibitors because of their characteristics of strong chemical activity and low toxicity [6-9]. Despite the large numbers of organic compounds, the choice of an appropriate inhibitor for a particular system is very limited due to the specificity of the inhibitors and the great variety of corrosion systems. Many derivatives of thiosemicarbazones are widely studied for their corrosion inhibition activity. In the present course of studies the corrosion inhibiting behavior of a novel Schiff base, thiophene-2-carbaldehydethiocarbamoylhydrazide (T2CTCH) was investigated on mild steel in 1M HCl solutions using weight loss measurement at different temperatures, electrochemical impedance spectroscopy (EIS) and potentiodynamic polarization analysis. Attempts were also made to propose the mechanism of inhibition of corrosion on mild steel and to correlate the experimentally derived data.

Experimental**Preparation of the Schiff Base**

Equimolar mixture of thiosemicarbazide and the aryl derivative of thiophene-2-carbaldehyde in ethanol medium was refluxed for 3 hours, concentrated and cooled. The pale yellow coloured Schiff base thiophene-2-carbaldehydethiocarbamoylhydrazide (T2CTCH) separated was filtered, washed with cold water and dried. Figure 1

represents the molecular structure of the heterocyclic Schiff base T2CTCH. Anal. calcd. for $C_{13}H_{11}N_3O_2S_2$: C 51.08, H 3.60, N 13.75, S 20.95 %. Found C 50.40, H 3.57, N 13.63, S 20.21%. IR (KBr): $\nu_{C=N}$ 1563cm^{-1} , $^1\text{H NMR}$: δ_{COOH} 12.8, $\delta_{\text{CH=N}}$ 9.84, $^{13}\text{C NMR}$: δ_{COOH} 182.98, $\delta_{\text{CH=N}}$ 131.5.

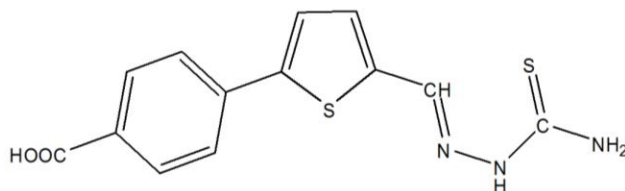


Figure 1 Molecular structure of T2CTCH.

Weight loss measurements

Mild steel (MS) specimens of dimension 1.5x 2x 0.1 cm were taken and abraded with various grades of silicon carbide papers. The specimens were then degreased with acetone, washed and dried. The area and thickness of MS plates were measured. After weighing, specimens were separately immersed in 50ml 1M HCl solution at 280C in the absence and presence of the inhibitor T2CTCH. After 24 hours weight loss of metal specimens were noted and this procedure was continued for five days. The experiments were carried out in duplicate and the average values are reported. The corrosion rate (v) is calculated by the following equation [10].

$$v = \frac{W}{St} \quad (1)$$

where W is the average weight loss of metal specimens, S is the total area of specimen and t is the time of treatment. The percentage of inhibition efficiency (η) was calculated using the equation.

$$\eta_w \% = \frac{v_0 - v}{v_0} \times 100 \quad (2)$$

where v_0 and v are the corrosion rates of uninhibited and inhibited specimens respectively[11].

Electrochemical impedance spectroscopic measurements (EIS)

The EIS measurements were performed in a three electrode assembly. Working electrode was prepared using the mild steel plate. A platinum gauze and a saturated calomel electrode (SCE) were used as the counter and reference electrode, respectively. EIS experiments were carried out on an Ivium compactstat-e-electrochemical system. 1M HCl was taken as the electrolyte and the working area of the metal specimens were exposed to the electrolyte for 1 h prior to the measurement. EIS measurements were performed at constant potential (OCP) in the frequency range from 1 KHz to 100 mHz with amplitude of 10mV as excitation signal. The percentage of inhibition from impedance measurements was calculated using charge transfer resistance values by the expression [12]

$$\eta_{\text{EIS}} \% = \frac{R_{\text{ct}} - R'_{\text{ct}}}{R_{\text{ct}}} \times 100 \quad (3)$$

where R_{ct} and R'_{ct} are the charge transfer resistances of working electrode with and without inhibitor respectively.

Potentiodynamic polarization studies

Electrochemical polarization plots were obtained by recording anodic and cathodic potentiodynamic polarization behavior. Polarization curves were obtained in the electrode potential range from -100 to +100 mV Vs corrosion potential (E_{corr}) at a scan rate of 1mV/sec. Tafel polarization analysis were done by extrapolating anodic and

cathodic curves to the potential axis to obtain corrosion current densities (I_{corr}). The percentage of inhibition efficiency ($\eta_{\text{pol}}\%$) was evaluated from the measured I_{corr} values using the relation [13]

$$\eta_{\text{pol}} \% = \frac{I_{\text{corr}} - I'_{\text{corr}}}{I_{\text{corr}}} \times 100 \quad (4)$$

where I_{corr} and I'_{corr} are the corrosion current densities of the exposed area of the working electrode in the absence and presence of inhibitor respectively. From the slope analysis of the linear polarization curves in the vicinity of corrosion potential of blank and different concentrations of the inhibitor, the values of polarization resistance (R_p) in 1M HCl solution were obtained. From the evaluated polarization resistance, the inhibition efficiency was calculated using the relationship

$$\eta_{R_p} \% = \frac{R'_p - R_p}{R'_p} \times 100 \quad (5)$$

where, R'_p and R_p represents the polarization resistance in the presence and absence of the inhibitor respectively [14].

Results and discussions

Weight loss measurements

In Table 1 the rates of corrosion of the MS specimens and inhibition efficiencies of different concentrations of T2CTCH and the parent amine is compared. It follows from the data that the weight loss decreased and therefore the corrosion inhibition is strengthened with increase in inhibitor concentration. This trend may result from the fact that adsorption and surface coverage increases with the increase in T2CTCH concentration and thus the surface is efficiently separated from the medium [15]. A maximum of 94.03% inhibition efficiency could be achieved by T2CTCH molecules at a concentration of 1.0 mM.

Table 1 The corrosion rate and percentage of inhibition efficiencies of T2CTCH and thiosemicarbazide for MS specimens immersed in 1M HCl at 28°C for 24 h.

Conc. (mM)	T2CTCH		Thiosemicarbazide	
	v (mm ^y - ¹)	$\eta_w\%$	v (mm ^y - ¹)	$\eta_w\%$
0	5.93	-	-	-
0.2	7.03	73.06	3.18	46.46
0.4	5.42	79.25	-	-
0.6	2.36	90.95	1.79	69.72
0.8	2.66	89.81	-	-
1.0	1.56	94.03	1.46	75.38

Adsorption isotherm and free energy of adsorption

The best fit adsorption isotherm for the adsorption of T2CTCH on MS specimens in 1M HCl was Langmuir adsorption isotherm which can be expressed as,

$$\frac{C}{\theta} = \frac{1}{K_{\text{ads}}} + C \quad (6)$$

where C is the concentration of the inhibitor, θ is the fractional surface coverage and K_{ads} is the adsorption equilibrium constant [16]. The Langmuir adsorption isotherm for T2CTCH is given in Figure 2 and the K_{ads} is related to the standard free energy of adsorption $\Delta G^{\circ}_{\text{ads}}$, by

$$\Delta G^{\circ}_{\text{ads}} = -RT \ln (55.5 K_{\text{ads}}) \quad (7)$$

where 55.5 is the molar concentration of water, R is the universal gas constant and T is the temperature in Kelvin [17]. The negative value of free energy of adsorption indicates the spontaneity of the process. $\Delta G^{\circ}_{\text{ads}}$ value upto -20 kJ mol^{-1} is an indication of the electrostatic interaction of the charged molecule and the charged surface of the metal (physisorption). In the present investigation, the T2CTCH molecules are having $G^{\circ}_{\text{ads}} = -16.12 \text{ kJ/mol}$ suggesting that the adsorption involves physisorption [18].

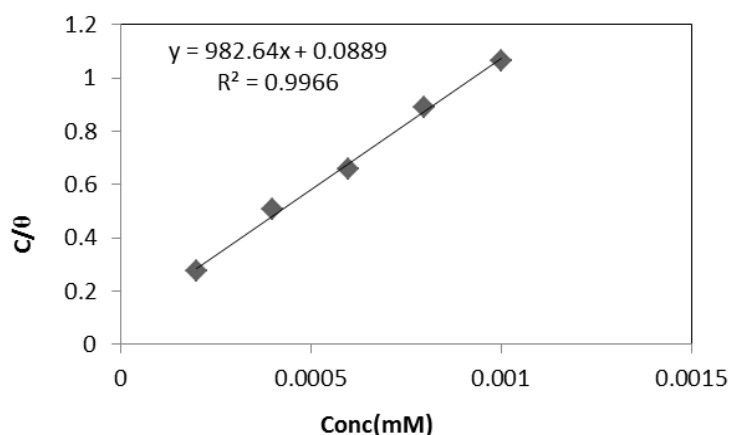


Figure 2 Langmuir adsorption isotherm for T2CTCH on MS surface in 1M HCl at 28°C

The mechanism of inhibition can be attributed to the adsorption of protonated Schiff base on the surface and hence reduce the dissolution of Fe to Fe^{2+} [19]. Besides this, the interaction of unshared electron pairs in the molecule with the metal and the interaction of π -electrons with the metal and a combination of these types are also possible. The unshared pair of electrons present on N atoms is of key importance in making coordinate bond with the metal. The π -electron cloud of the aromatic rings and the azomethine linkage also participate in the inhibition mechanism. Furthermore, the double bonds in the inhibitor molecule permit the back donation of metal d electrons to the π^* orbital and this type of interaction cannot occur with amines [20].

Effect of Temperature

The effect of temperature on corrosion rate was also evaluated using weight loss measurement in the temperature range of 30-60°C. The activation energy of corrosion with and without the inhibitor could be calculated by Arrhenius equation

$$K = A \exp\left(-\frac{E_a}{RT}\right) \quad (8)$$

where K is the rate of corrosion, E_a the activation energy, A the frequency factor, T the temperature in Kelvin scale and R is the gas constant. Figure 3 gives the linear plots between $\log K$ and $1000/T$ having regression coefficients close to unity which indicate that the corrosion of MS in HCl could be explained by the simple kinetic model. Enthalpy and entropy of activation (ΔH^* , ΔS^*) were calculated from the transition state theory

$$K = \left(\frac{RT}{Nh}\right) \exp\left(\frac{\Delta S^*}{R}\right) \exp\left(\frac{-\Delta H^*}{RT}\right) \quad (9)$$

where N is the Avogadro number and h is the Planks constant. A plot of $\log(K/T)$ Vs $1000/T$ in the presence and absence of the inhibitor is represented in Figure 4. Table 2 shows the activation energy and thermodynamic parameters of corrosion. The increase of activation energy of dissolution of the metal with increase in the inhibitor concentration implies the increase in the reluctance of dissolution of metal. Positive signs of enthalpies with a regular rise reflect the endothermic nature of dissolution and the increasing difficulty of corrosion with the inhibitor. The entropy of activation also increases with the inhibitor concentration. For the lower concentrations of the inhibitor, the entropy of activation is negative indicating that the activated molecules are in highly ordered state than that at the initial state. But as the concentration of inhibitor rises, the disordering of activated complex becomes more significant and the entropy of activation becomes positive.

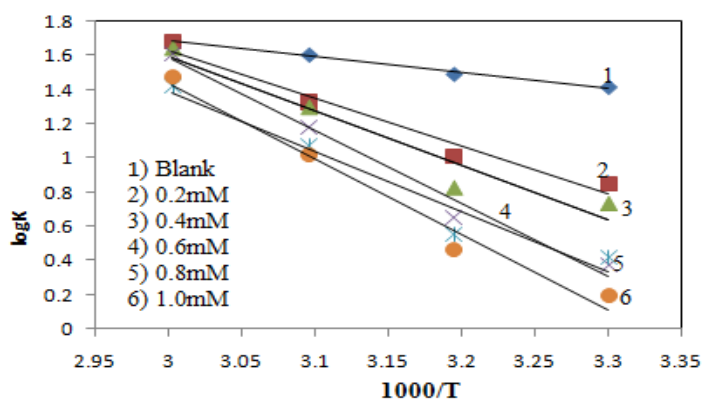


Figure 3 Arrhenius plots to calculate the activation energy

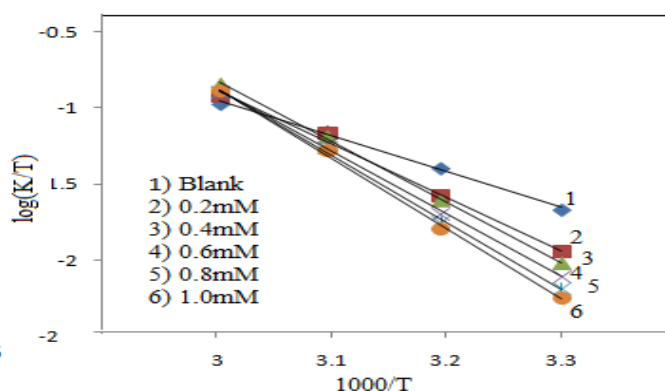


Figure 4 Plots of $\log(K/T)$ vs $1000/T$

Table 2 Thermodynamic parameters of corrosion of MS in 1 M HCl with and without the inhibitor T2CTCH

C (mM)	E_a (KJ mol ⁻¹)	A	ΔH^* (KJ mol ⁻¹)	ΔS^* (J mol ⁻¹ K ⁻¹)
Blank	17.57	1.13X10 ⁹	47.7	-24.22
0.2	53.96	1.2X10 ¹⁰	54.0	-4.572
0.4	61.29	1.58X10 ¹¹	61.3	16.87
0.6	67.15	7.94X10 ¹¹	67.1	30.27
0.8	81.87	2.57X10 ¹⁴	81.9	78.33
1.0	84.75	5.25X10 ¹⁴	84.7	84.27

Electrochemical impedance spectroscopy

The impedance responses of metal specimens are represented as Nyquist and Bode plots in Figure 3 and 4. There is a marked difference in the impedance behavior in the presence and absence of the inhibitor T2CTCH. The capacitance loop intersects the real axis at higher and lower frequencies. At high frequency end, the intercept corresponds to the solution resistance (R_s) and at lower frequency end, corresponds to the sum of R_s and charge transfer resistance (R_{ct}). The difference between the two values gives R_{ct} [21-23]. The value of R_{ct} is a measure of electron transfer across the exposed area of the metal surface and it is inversely proportional to rate of corrosion [24, 25].

The simple equivalent circuit that fit to many electrochemical system composed of a double layer capacitance, R_s and R_{ct} [26]. Impedance behavior can be well explained by pure electric models that could verify and enable to calculate numerical values corresponding to the physical and chemical properties of electrochemical system under examination. To reduce the effects due to surface irregularities of metal, constant phase element (CPE) is introduced into the circuit instead of a pure double layer capacitance [27] which gives more accurate fit as shown in the Figure 5.

The impedance of CPE can be expressed as $Z_{CPE} = \frac{1}{Y_0 (j\omega)^n}$ (10)

where Y_0 is the magnitude of CPE, n is the exponent (phase shift), ω is the angular frequency and j is the imaginary unit. CPE may be resistance, capacitance and inductance depending upon the values of n [28]. In all experiments the observed value of n ranges between 0.8 and 1.0, suggesting the capacitive response of CPE.

Table 3 Electrochemical Impedance parameters of MS specimens in 1M HCl in the absence and presence of T2CTCH

Conc (mM)	R_{ct} (Ωcm^2)	CPE (μFcm^{-2})	$\eta_{\text{EIS}}\%$
0	16.4	95.8	-
0.2	36.7	46.8	55.31
0.4	117	44.8	85.98
0.6	229	40.7	92.84
0.8	269	41.8	93.90
1.0	309	37	94.69

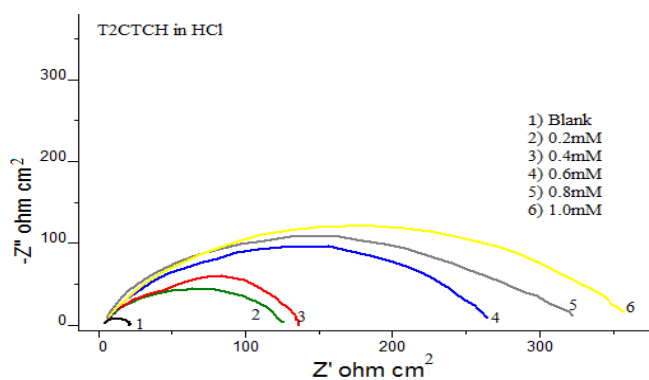


Figure 5 Nyquist plots for MS specimens in the presence and absence of T2CTCH

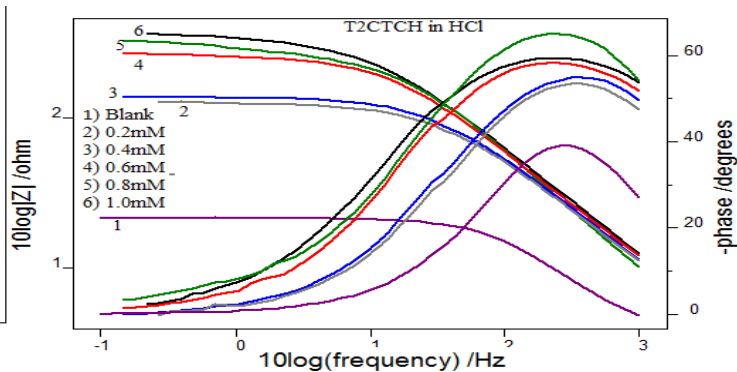


Figure 6 Bode plots of MS specimens in the presence and absence of T2CTCH

Table 3 lists the EIS parameters such as R_{ct} , R_s and CPE and the calculated values of percentage of inhibition ($\eta_{\text{EIS}}\%$) of MS specimens. R_{ct} values are increased with increasing inhibitor concentration. Decrease in capacitance values CPE with inhibitor concentration can be attributed to the decrease in local dielectric constant and/or increase in the thickness of the electrical double layer. This emphasizes the action of inhibitor molecules by adsorption at the metal-solution interface [29]. The percentage of inhibition ($\eta_{\text{EIS}}\%$) showed a regular increase with increase in inhibitor concentration. A maximum of 94.69% inhibition efficiency could be achieved at an inhibitor concentration of 1mM.

Potentiodynamic polarization studies: Potentiodynamic polarization plots obtained for T2CTCH are shown in Fig. 6. In Table 3 polarization parameters like corrosion current densities (I_{corr}), corrosion potential (E_{corr}), cathodic Tafel

slope (b_c), anodic Tafel slope (b_a), and inhibition efficiency (E_p) for MS specimens are listed. In the presence of the inhibitor T2CTCH there is a prominent decrease in the corrosion current density (I_{corr}). The inhibitor solution of concentration 1 mM exhibited a maximum inhibition efficiency of 97.15% with the lowest value of I_{corr} . Since the value of b_a changes appreciably in the presence of T2CTCH, it may be assumed that the inhibitor molecules are more adsorbed on anodic sites. Generally if the shift of E_{corr} is >85 with respect to E_{corr} of uninhibited solution, the inhibitor can be viewed as cathodic or anodic type [30]. Since in the present study the maximum shift of E_{corr} is 48mV, it can be suggested that T2CTCH acts as a mixed type inhibitor for MS specimens in 1M HCl [31].

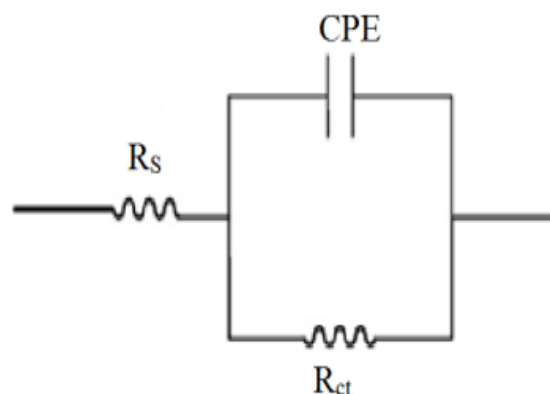


Figure 7 Equivalent circuit fitting for EIS measurements

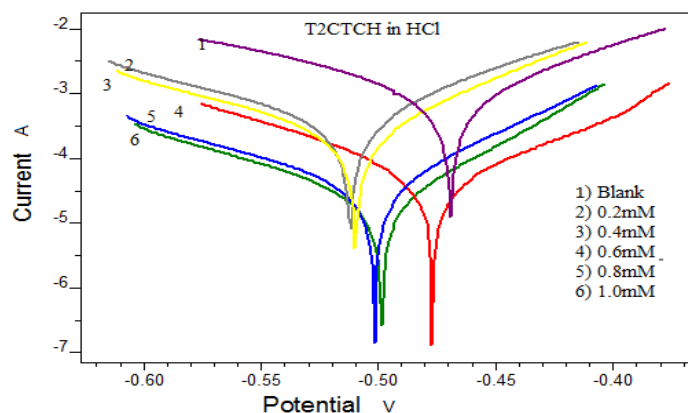


Figure 8 Tafel plots of MS Specimens with and without inhibitor T2CTCH

Table 4 Potentiodynamic polarization parameters of MS specimens in 1M HCl at 28°C in the absence and presence of T2CTCH

Conc. (mM)	Tafel Data					Linear polarization data	
	E_{corr} (mV/SCE)	I_{corr} ($\mu\text{A}/\text{cm}^2$)	b_a (mv/dec)	$-b_c$ (mV/dec)	$\eta_{pol}\%$	R_p (ohm)	$\eta_{Rp}\%$
0	-465	726	72	106	-	21.8	-
0.2	-510	316	63	103	56.47	47.59	54.19
0.4	-512	204	72	105	71.90	68.78	68.30
0.6	-502	32.6	58	99	95.51	423	94.85
0.8	-513	29.1	70	90	95.99	504	95.67
1.0	-499	20.7	51	94	97.15	619	96.48

Conclusions

1. T2CTCH is a good inhibitor for MS in 1M HCl. A maximum of 94% of inhibition efficiency could be achieved with this inhibitor by weight loss measurements.
2. Compared to the parent amine thiosemicarbazide, the Schiff base T2CTCH exhibited higher inhibition efficiency.
3. The inhibition mechanism is explained by adsorption. Adsorption of Schiff base on MS surface obey Langmuir isotherm.
4. The thermodynamic parameters of the adsorption calculated from the adsorption isotherm showed that physisorption is involved in the inhibition process.

References

- [1] N.N. Greenwood, A. Earnshaw, Chemistry of the Elements, Pergamon Press, Oxford, England. 1984.
- [2] H. Harms, H. P. Volkland, G. Repphun, A. Hiltolt, O. Wanner, and A.J.B. Zehnder; Corros. Sci., 2003, 45, 1717.
- [3] H.H. Hassan, Electrochim. Acta 2005, 51, 526.
- [4] A. Lalitha, S. Ramesh and S. Rajeswari, Electrochim. Acta, 2005, 51, 47.
- [5] F. Bentiss, M. Bouanis, B. Mernari, M. Traisnel, H. Vezin and M. Lagrenée, Appl. Surf. Sci., 2007, 253, 3696.
- [6] M. Lebrini, F. Bentiss, H. Vezin and M. Lagrenée; Appl. Surf. Sci., 2005, 252, 950.
- [7] M. Bouklah, B. Hammouti, M. Lagrenée and F. Bentiss; Corros. Sci., 2006, 48, 2831.
- [8] F. Bentiss, M. Lagrenée, M. Traisnel and J.C. Hornez, Corrosion, 1999, 55, 968.
- [9] F. Bentiss, M. Traisnel, H. Vezin, H.F. Hildebrand and M. Lagrenée, Corros. Sci., 2004, 46, 2781.
- [10] Shuduan Deng, Xianghong Li and Hui Fu; Corros. Sci., 2011, 53, 3596.
- [11] ASTM G-31-72, Standard recommended practice for the laboratory immersion corrosion testing of metals, ASTM, Philadelphia, 1990, 401.
- [12] K.C. Emregul, O. Atakol; Materials Chemistry and Physics, 2004, 893, 373.
- [13] H. Ashassi-Sorkhabi, B. Shaabani and D. Seifzadeh; Electrochim. Acta, 2005, 50, 3446.
- [14] A. Raman and P. Labine, Reviews on Corrosion Inhibitor Science and Technology, NACE, Houston, Tex, USA, 1986.
- [15] T. Zhao, G. Mu, Corros. Sci. 1999, 41, 1937.
- [16] E. Cano, J.L. Polo, A. La Iglesia and J.M. Bastidas; Adsorption, 2004, 10, 219.
- [17] X. Li, S. Deng, and H. Fu; Corrosion Science, 2009, 51, 1344.
- [18] Aby Paul, K. Joby Thomas, Vinod P. Raphael and K.S. Shaju; Oriental Journal Of Chemistry, 2012, 28, 1501.
- [19] Vinod P. Raphael, K. Joby Thomas, K.S. Shaju and Aby Paul; Research On Chemical Intermediates, 2013, 39.
- [20] E. Cano, J.L. Polo, A. La Iglesia and J.M. Bastidas; Adsorption, 2004, 10, 219.
- [21] H. H. Hassan, E. Abdelghani, M. A. Amin; Electrochimica Acta, 2007, 52, 6359.
- [22] F. Mansfeld, Corrosion, 1981, 39, 301.
- [23] M.S. Abdel-Aal, M.S. Morad; British Journal of Corrosion, 2011, 36, 253.
- [24] P. Bommersbach, C. Alemany-Dumont, J.P. Millet and B. Normand; Electrochimica Acta, 2005, 51, 1076.
- [25] I.L. Rosenfield, Corrosion Inhibitors, McGraw-Hill, New York, 1981, 66.
- [26] M. El Azhar, B. Mernari, M. Traisnel, F. Bentiss and M. Lagrenée; Corrosion Science, 2001, 43, 2229.
- [27] A. Yurt, A. Balaban, S. U. Kandemir, G. Bereket, B. Erk; Materials Chemistry and Physics, 2004, 85, 420.
- [28] A. K. Singh, S. K. Shukla, M. Singh and M.A. Quraishi; Materials Chemistry and Physics, 2011, 129, 68.
- [29] E. McCafferty, Norman Hackerman; Journal of Electrochemical Society, 1972, 119, 146.
- [30] F. Bentiss, M. Lebrin and M. Lagrenée; Corrosion Science 2005, 47, 2915.
- [31] West D. X., Carison C. S., Liberta A. E., Albert J. N. and Daniel C. R., Transition Metal Chemistry, 1990, 15, 341.

© 2014, by the Authors. The articles published from this journal are distributed to the public under “**Creative Commons Attribution License**” (<http://creativecommons.org/licenses/by/3.0/>). Therefore, upon proper citation of the original work, all the articles can be used without any restriction or can be distributed in any medium in any form.

Publication History

Received 25th Oct 2014
Revised 14th Nov 2014
Accepted 21st Nov 2014
Online 30th Nov 2014